

Preliminary Analysis of OGLE-2007-BLG-472

Noé Kains*, K.Horne, M.Dominik, the PLANET collaboration

SUPA, University of St Andrews

E-mail: nk87@st-andrews.ac.uk

We present the analysis of the anomalous microlensing event OGLE-2007-BLG-472, including a fit of a binary lens model to the data. This event is a low-magnification and highly blended event with a pair of caustic crossings separated by 2.7 days. From our best-fit model and a chosen Galactic model, we derive Bayesian probability densities for physical properties of the planet and its host star. We derive a secondary mass of $9.74^{+11.70}_{-5.34} M_J$, which lies near the formal frontier between the planetary and brown dwarf mass regimes ($13 M_J$)

The Manchester Microlensing Conference: The 12th International Conference and ANGLES Microlensing Workshop

January 21-25 2008

Manchester, UK

*Speaker.

1. Introduction

Since the first extrasolar planet detection in 1995, several major collaborations have formed to coordinate the observational effort needed to detect exoplanets. Among the different techniques used, gravitational microlensing is most sensitive in low-mass and larger orbital radius ranges (1-5 AU), with radial velocity, transit and astrometry methods favouring planets that are in close-in orbits around their host star. This is due to the high signal-to-noise ratio of the perturbation caused by even low-mass companions to stellar lenses.

Microlensing collaborations currently function with collaborations issuing early warnings of candidate microlensing events, and selected promising events being more intensely observed by follow-up collaborations. Among these, the PLANET collaboration monitors events alerted by the OGLE and MOA collaborations, using telescopes at 6 different sites, covering a wide range of longitudes. This resulted in the discovery in 2005 of a 5.5 Earth masses planet, the lowest mass extrasolar planet discovered to date (Beaulieu et al 2006). As of November 2007, four robust detections of extrasolar planets by microlensing have been confirmed, with several additional candidates observed during the 2007 season, including the event presented in this paper.

2. Microlensing

Microlensing events occur when the light rays of a source star are bent in the gravitational field of a foreground 'lens' star, leading to an apparent brightening of the source. They occur when the angular separation of the lens and source stars is of the order of the *angular Einstein radius* θ_E , and can be described analytically with three parameters: the time of closest source-lens approach t_0 , the Einstein radius crossing time t_E and the source-lens separation at closest approach u_0 (in units of θ_E). When a secondary companion is orbiting the lens star, the companion perturbs the single-lens magnification map through the presence of caustics, regions of space where the magnification of the source diverges to infinity for a perfect point source. The presence of these caustics lead to observed perturbations if the source star passes close enough to them. While this happens on a random basis for planetary caustics, in the case of high-magnification events (i.e. when the minimum projected source-lens angular separation is small), the source will *always* pass close to the central caustic, because central caustics are located around the host star's position. Therefore high-magnification events alerted by early warning systems are prime events to be selected for observing by follow-up collaborations.

Lensing by a system of multiple lenses can be described by the multiple lens equation (e.g. Schneider & Weiss 1992), which for a collection of N masses m_i at positions d_i is written

$$\mathbf{x} - \mathbf{y} - \sum_{i=1}^N m_i \frac{\mathbf{x} - d_i}{|\mathbf{x} - d_i|^2} = 0 \quad (2.1)$$

where the positions of the images and source in the lens plane is expressed by complex numbers \mathbf{x} and \mathbf{y} following the formalism of Witt (1990). Although this equation cannot be solved analytically, there are various ways to solve it numerically, including writing a complex polynomial equation by eliminating \mathbf{x}^* , the complex conjugate of \mathbf{x} , from Eq.(2.1), and keeping the solutions of this equation which are also solutions of the lens equation. For a binary-lens ($N=2$) case, this

approach yields a fifth-order complex polynomial equation, as shown by Witt & Mao (1995). The magnification of a source star by a binary lens can be fully described by 7 model parameters. These are the three single lens parameters t_0 , t_E and u_0 , as well as the source trajectory's angle with the axis going through both components of the lens, α ; the source size in units of (the lens') Einstein ring radii, ρ_* , the distance between the two lens components in unit of the Einstein radius, d , and q , the mass ratio of the two components.

3. OB07472

On 19 August 2007, the OGLE Early Warning System flagged microlensing candidate event OGLE-2007-BLG-472 at right ascension $\alpha = 17:57:04.34$, and declination $\delta = -28:22:02.1$.

The OGLE lightcurve has a baseline magnitude $I=16.00$. Lensing by the star in the point source-point lens (PSPL) approximation causes a broad rise and fall in the lightcurve, peaking around $\text{MJD}^1=4334.0$ with half-width at half-peak of about 10 days. Although the observed OGLE flux rises only by 0.15 mag, the shape of the lightcurve indicates a high blending, with only $\sim 12\%$ of the baseline flux due to the un-magnified source. As a result, the peak PSPL magnification is actually higher, at $A_0=1.67$, corresponding to -0.55 mag. Comparing PSPL fits excluding the anomaly and with and without accounting for the blended flux, the event timescale obtained from the fit increases from $t_E=9.02$ days to 15.35 days, and increases the peak magnification from $A_0=1.39$ to 1.67.

At $\text{MJD}=4331.5$ an OGLE data point showed sudden brightening of the source, with subsequent PLANET (UTas Mt. Canopus 1.0m telescope in Tasmania and Danish 1.54m at La Silla, Chile) and OGLE data indicating what appears to be a fold caustic crossing by the source, ending with a PLANET UTas data point at $\text{MJD}=4334.1$. The caustic entry is observed by a single OGLE point, while the caustic exit is well covered by UTas our data set. The base PSPL curve then reached peak magnification at $\text{MJD}=4335.45$ (August 22). As shown in the analysis below, the caustic crossing is caused by the presence of a companion to the lens with a mass lying near the formal end of the mass planetary range. This limit is defined by the International Astronomical Union as the mass below which thermonuclear fusion of deuterium cannot take place, and is calculated to be approximately 13 Jovian Masses (e.g. Basri 2003).

From features of the lightcurves, we make estimates for the values of some of the parameters. Comparing the duration of the anomaly $\Delta t=2.6$ days with the event timescale t_E , we get an estimate for the mass ratio of $q \sim (\frac{\Delta t}{t_E})^2 \sim 0.03$. The 15-day event timescale suggests the lens star is an M dwarf, with $M/M_\odot \sim 0.3$, giving a planet mass $M_P = qM \sim 9M_j$.

We used a Markov Chain-Monte Carlo algorithm to fit the data from OGLE and the two PLANET sites, starting the algorithm at many different values to ensure good coverage of the parameter space. Particularly crucial in our data set is the UTas observation taken within a few hours of the caustic exit, which puts strong constraints on the position of the caustic on the lightcurve, and also puts upper constraints on the source size. The last data point inside the caustic and the first data point after the caustic exit enable us to determine the maximum source radius crossing time t_* . Since this directly relates to the source size through $\rho_* = t_*/t_E$, we can use a conservative value

¹MJD=HJD-2450000

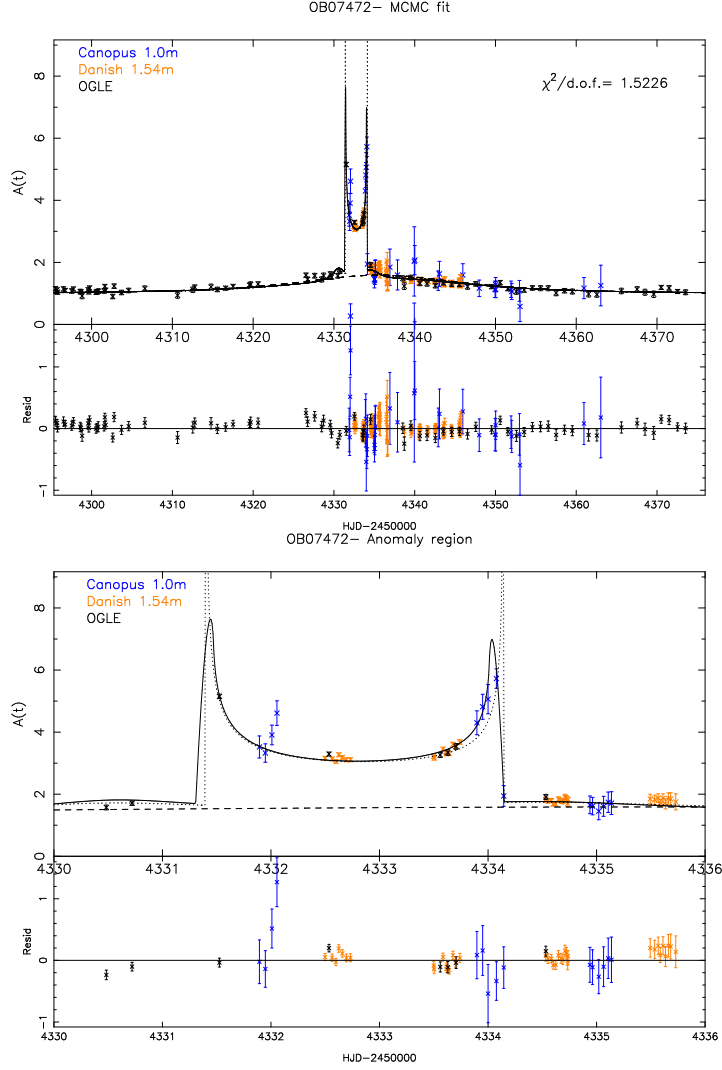


Figure 1: Best-fit binary lens model for microlensing event OGLE-2007-BLG-472 with a zoom on the anomaly (bottom panel). Data points are plotted with $1\text{-}\sigma$ error bars. The Canopus data error bars have been rescaled by a factor of $\sqrt{34.4}$. The dashed line is the best-fit point source - point lens model. The dotted line is the best binary-lens model with zero source size.

of t_E to determine the maximum possible source radius. Using $t_E = 13$ days, we get a maximum value of ρ_* of 0.005 (in units of the Einstein Ring radius).

If we rescale the UTAs error bars to obtain a value of χ^2 per degree of freedom for this data set equal to 1 in early models obtained with nominal error bars and refit our data with these new error bars, we obtain the best-fit sets of parameters given in Tables 1 & 2.

4. Characteristics of the planetary model

Although the characteristics of any microlensing event depends on various properties of the lensing system, including the mass of the lens, the only measurable quantity that can be directly related to physical properties of the lens is the timescale of the event t_E . All other properties

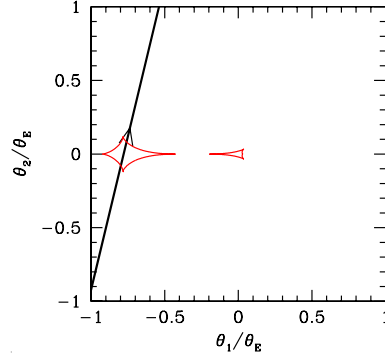


Figure 2: The trajectory of the source in the lens plane with the caustics. The primary lens component is located at $\theta_1 = \theta_2 = 0$.

Parameter	Best-fit value	Units
χ^2	1429.47/968	—
$\chi^2_{\text{UTas}}/\text{no. of points}$	20.89/32	—
$\chi^2_{\text{Danish}}/\text{no. of points}$	106.39/79	—
$\chi^2_{\text{OGLE}}/\text{no. of points}$	1302.19/857	—
t_0	4335.873 ± 0.185	MJD
t_E	17.063 ± 0.771	days
α	1.333 ± 0.014	rad
u_0	0.767 ± 0.021	—
A_0	1.58 ± 0.06	—
ρ_*	0 (fixed)	θ_E
d	1.481 ± 0.015	R_E
q	0.025 ± 0.003	—

Table 1: Best fit binary lens model parameters with rescaled UTas error bars

Parameter	Best-fit value	Units
χ^2	1454.08/968	—
$\chi^2_{\text{UTas}}/\text{no. of points}$	22.95/32	—
$\chi^2_{\text{Danish}}/\text{no. of points}$	113.76/79	—
$\chi^2_{\text{OGLE}}/\text{no. of points}$	1317.37/857	—
t_0	4335.647 ± 0.151	MJD
t_E	16.126 ± 0.664	days
α	1.335 ± 0.0173	rad
u_0	0.757 ± 0.019	—
A_0	1.59 ± 0.07	—
ρ_*	0.0036 ± 0.0006	θ_E
d	1.476 ± 0.015	R_E
q	0.026 ± 0.004	—

Table 2: Best fit binary lens model parameters with rescaled UTas error bars

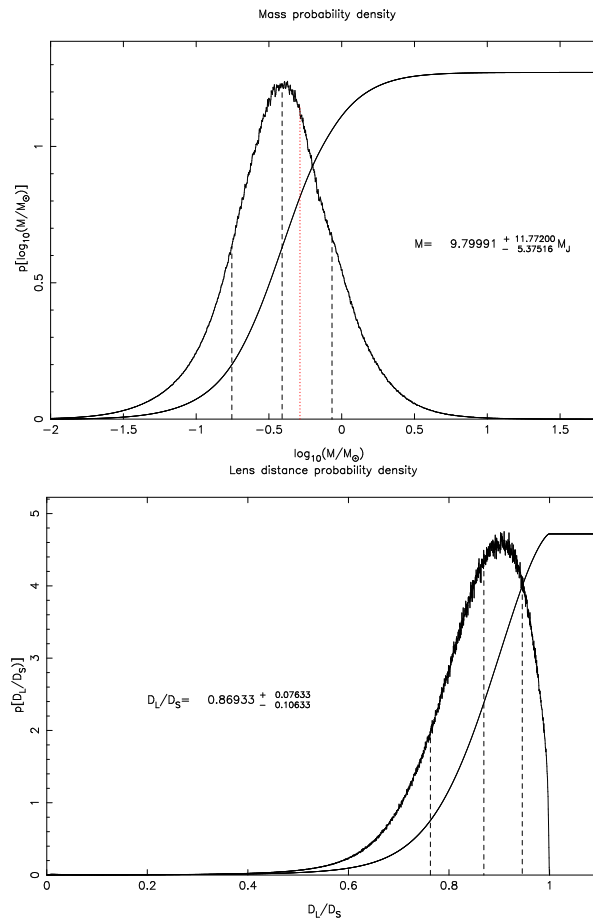


Figure 3: Probability densities for the mass of the host star and the fractional distance D_L/D_S . The values quoted are the median value and the limits of the 68.3% confidence interval, which are shown on the plot as dashed lines. The dotted line on the mass probability density plot indicates the end of the planetary mass range at 13 Jovian masses.

can then only be determined using Bayesian inference, based on a chosen Galactic model. Using a probabilistic approach following that of Dominik 2005, we derive probability densities for physical properties of the planet and its host star. The Galactic model used here is a piecewise present-day mass spectrum (e.g. Chabrier 2003), two double exponentials for the disk mass density and a barred bulge tilted at an angle of 20° with the direction to the Galactic centre (Dwek et al. 1995), and the distribution of effective transverse velocities used in Dominik 2005. Probability densities for the mass of the host star and its position between the observer and the source derived using these models are plotted on Figure 4. From distributions based solely on t_E , we infer a planetary mass $M = 9.74_{-5.34}^{+11.70} M_J$ Jovian masses, at a fractional distance $\frac{D_L}{D_S} = 0.87_{-0.11}^{+0.08}$, or a distance $D_L = 7.39_{-0.90}^{+0.65}$ kpc for a bulge source located at 8.5 kpc.

5. Alternative models

Apart from the zero source size model mentioned above, the relatively poor event coverage and some of the data points mean that alternative models with similar values of the goodness-of-fit

Model #	Best-fit value of q	χ^2
Nominal error bars, point source	0.0309 ± 0.0004	2084.89
Nominal error bars, extended source	0.0333 ± 0.0004	2093.60
Rescaled UTas error bars, point source	0.025 ± 0.003	1429.47
Rescaled UTas error bars, extended source	0.026 ± 0.004	1454.08
Alternative 1, rescaled UTas	0.998 ± 0.012	1609.63
Alternative 2, rescaled UTas	0.240 ± 0.001	1625.33

Table 3: Best fit parameters for alternative model # 1

statistics may exist. In particular, the similarity of this event with some earlier ambiguous events, especially OGLE #7 (Udalski 94), tells us that models with higher mass ratios may exist. As a test for other models, we take the different solutions proposed for the event OGLE #7 as starting points for our MCMC algorithm. The χ^2 values for each converged model are given in Table 3. Features in our current best-fit models that do not appear clearly in our data sets suggest that there may be better-fitting models. We therefore need to systematically explore our parameter space to find and characterise such alternative models.

6. Summary

Despite mediocre observational coverage and high blending, a few crucial data points enable us to find a preliminary binary-lens model fit to our data for OGLE-2007-BLG-472. While the best-fit mass ratio is high and would place the secondary component of the lens in the range of brown dwarf masses for a solar-mass primary component, the short duration of the event hints to a low lens mass, leaving the mass of the secondary component within the planetary mass regime. When issues in our photometry are solved it will be necessary to thoroughly explore the binary lens parameter space in order to find possible alternative models.

References

- [1] Basri G. & Brown M.E., *Annu. Rev. Earth Planet. Sci* 2006, 34:193-216
- [2] Beaulieu J.-P. et al., *Nature* 439, 437, 2006
- [3] Chabrier G., 2003, *PASP*, 115, 763
- [4] Dominik M., 2005 *MNRAS*, 367, 669
- [5] Dominik M., 2007, *MNRAS*, 377, 1679
- [6] Dwek E. et al., 1995, *ApJ*, 445, 716
- [7] Schneider P. & Weiss A., *A&A*, 260, n.1-2, pp.1-13, 1992
- [8] Udalski A. et al., *ApJ.*, 436, L103, 1994
- [9] Udalski A., *Acta Astron.*, 53, 291, 2003
- [10] Witt H.J. & Mao S., *ApJ*, vol.430, p.505, 1994
- [11] Witt H.J., *A&A* 236, n.2, pp.311-322, 1990